Host-Guest Systems | Hot Paper

Unlocking a (Pseudo)-Mechanically Interlocked Molecule with a Coronene "Shoehorn"

Susana Ibáñez[+], Katarzyna Świderek[+], and Eduardo Peris*

Abstract: Mechanically interlocked molecules (MIMs) have gained increasing interest during the last decades, not only because of their aesthetic appeal, but also because their unique properties have allowed them to find applications in nanotechnology, catalysis, chemo-sensing and biomedicine. Herein we describe how a pyrene molecule with four octynyl substituents can be easily encapsulated within the cavity of a tetragold(I) rectangle-like metallobox, by template formation of the metallo-assembly in the presence of the guest. The resulting assembly behaves as a mechanically interlocked molecule (MIM), in which the four long limbs of the guest protrude from the entrances of the metallobox, thus locking the guest inside the cavity of the metallobox. The new assembly resembles a metallo-suit[4]ane, given the number of protruding long limbs and the presence of the metal atoms in the host molecule. However, unlike normal MIMs, this molecule can release the tetra-substituted pyrene guest by the addition of coronene, which can smoothly replace the guest in the cavity of the metallobox. Combined experimental and computational studies allowed the role of the coronene molecule in facilitating the release of the tetrasubstituted pyrene guest to be explained, through a process that we named "shoehorning", as the coronene compresses the flexible limbs of the guest so that it can reduce its size to slide in and out the metallobox.

Introduction

Inspired by nature's ability interact selectively with small molecules, scientists have made a great effort to design artificial hosts molecules that mimic host–guest binding in bio-molecular events. In most cases, the high specificity
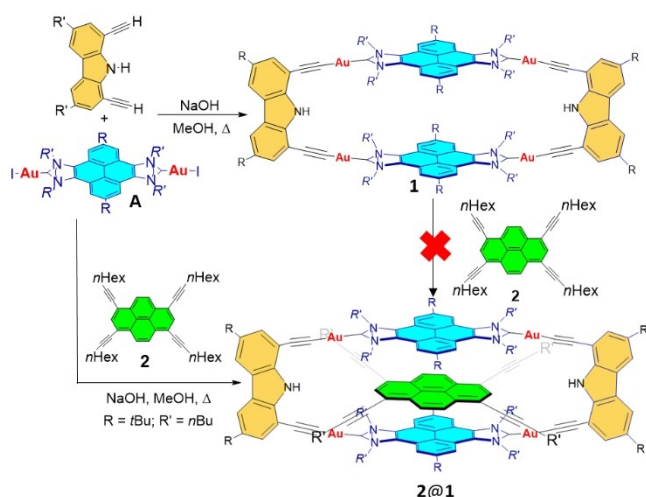
shown by enzymes is explained by their ability to modulate access to the active size by producing conformational changes which are referred to as "gating". Gating can also be observed in some artificial hosts, which can also bind and release guest molecules at rates that depend on conformational changes in their structures.[1] Gating was first described in artificial hosts by Houk and co-workers,[2] as a result of computational investigations on Cram's hemicarcerands.[3] Guest molecules trapped within the cavity of a hemicarcerand can be released without breaking covalent bonds when the system is heated at high temperatures. Other than temperature, the opening and close of gates in artificial hosts can also be controlled by applying redox or photochemical stimuli.[4] In any case, the structural conformational changes that facilitate guest encapsulation are normally observed in hosts, rather than in guests, because these changes require a high degree of flexibility that is more likely to be found in (large) hosts than in (small) guests. Unlike hemicarcerands, guest molecules encapsulated in carcerands cannot be released without breaking covalent bonds of the host molecule. Closely related to carcerands, Mechanically Interlocked Molecules (MIMs) consist of an entanglement of non-covalently bound subcomponents that cannot be separated without breaking covalent bonds between atoms.[5] MIMs such as catenanes,[6] rotaxanes[6a,b,f,7] and molecular knots[8] have gained increasing interest during the last decades, not only due to their aesthetic appeal, but also because their unique properties have allowed them to find applications in nanotechnology,[9] catalysis,[10] chemosensing[11] and biomedicine.[12]

We recently described a tetragold (I) metallorectangle built with two pyrene-bis-imidazolylidene ligands and two carbazolyl-bis-alkynyl linkers (**1**, Scheme 1), which we used for the encapsulation of a variety of polycyclic aromatic hydrocarbons (PAHs).[13] In the preparation of this metallobox, we observed that the product yield increased significantly when the synthesis was carried out in the presence of electron-rich PAHs,[13a] thus strongly suggesting that the formation of the cage can be guided by templation.[6g,14] We speculated that a similar strategy could be applied to the preparation of suitanes[15] (or pseudo-suitanes, as will be discussed below), if PAHs functionalized with four long limbs were used as templates in the preparation of this tetragold metallobox. The resulting structure would be constituted by a suit with two large portals from which four long limbs protruded, thus representing a unique type of metal-containing suit[4]ane-like molecule. However, contrary to what would be expected for a MIM, the tetrasubstituted guest can be replaced smoothly by large PAH molecules

[*] Dr. S. Ibáñez,[+] Dr. K. Świderek,[+] Prof. E. Peris
    Institute of Advanced Materials (INAM), Universitat Jaume I
    Av. Vicente Sos Baynat s/n. 12071 Castellón (Spain)
    E-mail: eperis@uji.es

[+] These authors contributed equally to this work.

Scheme 1. Synthesis of **2@1**.

Figure 1. Selected region of the ^{1}H NMR spectra (500 MHz, 298 K, CDCl$_3$) of **1** (a), **2** (b) and **2@1** (c).

(coronene or perylene), via a process that involves important conformational changes of the tetra-alkylated guest. While conformational changes on hosts for preventing/facilitating guest encapsulation release are well documented (gating), we are unaware that similar stimuli-response conformational changes on the guest have been utilized to unlock mechanically interlocked molecules. Herein, we describe the strategy to obtain a MIM-like molecule, and its unusual properties, which are derived from the flexible nature of the limbs of the guest.

Results and Discussion

Compound **2@1** was obtained according to the one-step synthetic procedure depicted in Scheme 1. The reaction of di-*tert*-butyl-diethynyl-carbazole with NaOH in refluxing methanol followed by the addition of the pyrene-bis-imidazolydene-di-gold(I) complex **A**,[16] in the presence of one equivalent of **2** afforded the inclusion complex **2@1** in 88 % yield. This product yield is remarkable, especially if we compare it with all other suitane-like molecules that have been reported so far, which are obtained in much lower yields (7–13 %).[15,17] The diffusion ordered spectroscopy (DOSY) spectrum of **2@1** shows that the two subcomponents of the inclusion complex have the same diffusion rate constant $(5.25 \times 10^{-10}\ \mathrm{m^2\,s^{-1}})$, and that this is significantly smaller than the diffusion coefficients found for the free molecules **1** and **2**, in agreement with the larger size of **2@1** (see Supporting Information for details). Figure 1 shows the ^{1}H NMR spectra of **1**, **2** and **2@1**, from which a clear evidence of the efficiency of the complexation can be derived. As can be observed in the spectrum of **2@1**, the signals due to the protons of the pyrene panels of the host (A) are considerably shielded, and consequently they experience a significant upfield shift, compared to the situation shown for the free host **1**. The resonance due to the protons of the NH groups (B) is shifted downfield. In
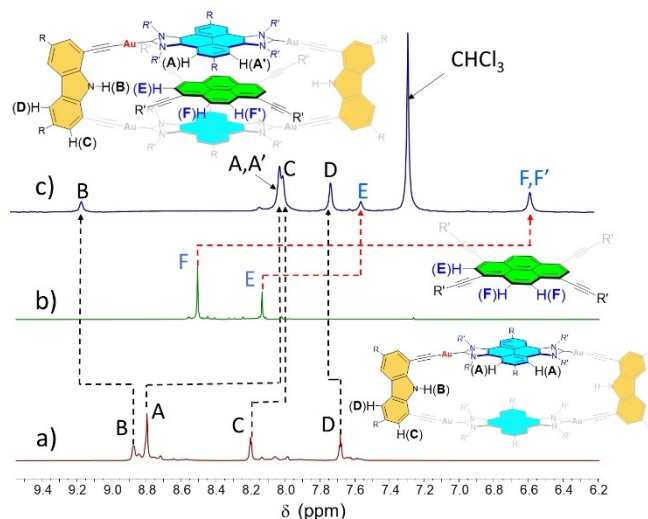
addition, the signals due to the pyrene protons of the pyrene tetra-octynyl guest in **2@1** are significantly shifted upfield (E and F). These observations are a clear indication of the existence of an effective π-π-stacking interaction between the pyrene core of the guest and the pyrene panels of the metallobox host.

We think that **2@1** is best described as a suitane, since the molecule consists of a metallobox that acts as a suit-like host with a torso-like guest with four protruding limbs, thus perfectly fitting to the well-accepted definitions of suitane.[15] Given that this assembly is constructed using a metal-loassembly strategy, we think that the term *metallo-suit-[4]ane* (or pseudo-metallo-suit[4]ane, as will be explained later) can be considered appropriate. The introduction of the metal into the structure of this molecule is important, as the directional control of metal-ligand binding facilitates the preparation of the resulting MIM in shorter reaction times and significantly higher yields compared to all other suitanes reported so far. However, our suitane molecule differs from all previously reported ones in that the four limbs of the guest protrude from the host by four effective (but not isolated) apertures. At this point, it is important to mention that the well-accepted definitions of suitanes do not specify that a coincidence between the number of protruding limbs and number of apertures is needed. In our case, the metallobox host contains two large apertures, each one divided in two 'effective' smaller apertures, which are separated by the bulky *tert*-butyl groups that decorate the pyrene moieties of the host.

The Uv/vis spectrum of **2@1** shows a broad absorption band centered at about 300 nm, together with lower energy bands (340–400 nm), which are attributed to the π-π transitions of the polyaromatic guest (Figure S15 in Supporting Information). The emission spectrum of **2@1** shows two bands centered at 425 and 475 nm, which may be attributed to the emission of the pyrene moieties of the metallobox

and the guest, respectively. The emission due to the guest is significantly redshifted compared to the related band shown by the free guest, as a consequence of the π-π stacking interaction with the metallobox (Figure S16 in Supporting Information). Compound **2** is a highly emissive molecule, with a quantum yield of 0.952, but its emission is significantly quenched when encapsulated in **1**, as reflected by the low quantum yield shown by **2@1** (0.288, as shown in Figure S17 in Supporting Information).

Complex **2@1** is stable at room temperature in $C_2D_2Cl_4$ solution for almost unlimited periods of time, without showing decomposition or any tendency to separate their subcomponent parts. Complex **2@1** also showed to be stable after being heated in $C_2D_2Cl_4$ solutions at 80°C for four hours. Only after the solution was heated at 80°C for several weeks, we observed that the metallobox **1** started to decompose, with the concomitant release of the tetrasubstituted pyrene **2** (Figure S9 in Supporting Information). This experiment indicates that the release of the guest is only produced after the cleavage of covalent bonds of the host, thus strongly supporting the interlocked nature of the system. In order to further confirm the interlocked nature of **2@1**, we performed one further experiment. We mixed the empty metallobox **1** with **2** in $C_2D_2Cl_4$ and heated the mixture for five days at 80°C. After this time, we observed that the inclusion complex **2@1** and was not formed, as the ^1H NMR spectrum of the resulting mixture was the superimposed spectra of free **1** and **2**. This experiment further confirms that **2@1** is not in equilibrium with a mixture of its subcomponents **1** and **2**, and therefore gives further support to the mechanically interlocked nature of **2@1**.

The molecular structure of **2@1** was confirmed by single crystal X-ray diffractometry (Figure 2).[18] The structure confirms that the tetra-octynyl-pyrene *torso* is sandwiched between the two pyrene platforms of the metallobox. The average distance between the pyrene moiety of the guest and the pyrene panels o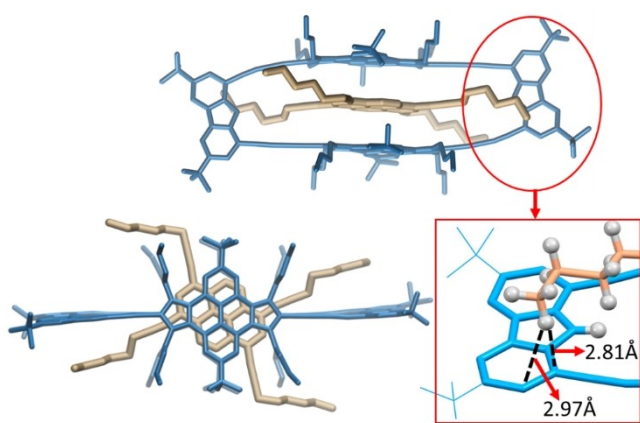f the host is 3.48 Å, thus indicating a high degree of attractive π-π stacking interaction. The centroids of the two pyrene panels of the metallobox and the pyrene moiety of the encapsulated guest are perfectly aligned, but the longest axis of the pyrene moiety of the guest is not aligned with the longest axis of the metallobox, as it was for the structure of pyrene@**1**, which we reported in a previous study.[13a] This deviation is 22.50° (measured as the dihedral angle between the two previously mentioned axles) and renders a situation in which two of the protruding limbs of the guest are closer to the carbazolyl spacer of the metallobox than the two other remaining ones. This situation reveals the most favorable accommodation of the tetra-substituted pyrene guest within the cavity of the host, in which the four limbs of the guest protrude from the cage through the less sterically hindered tunnels, which are located in the spaces defined between *n*-butyl groups of the imidazolylidenes and the carbazolyl spacer, and between the same *n*-butyl groups and the *tert*-butyl groups of the pyrene moieties of the metallobox, as can be clearly observed in the bottom structure shown in Figure 2. A perfect alignment between the longest axles of the pyrene-imidazolylidene ligands of the cage and the pyrene moiety of the host would render a sterically-hindered situation, since the alkynyl substituents of the guest would be aligned with the *n*-butyl groups of the host. Another interesting feature of the structure is that the terminal methyl groups of two of the alkyl chains of the guest are disposed close to one of the phenyl rings of the carbazolyl linker, so that the distance between one of the hydrogen atoms of the methyl group and two of the carbons of the phenyl group of the linker are 2.81 and 2.97 Å (See Figure 2), thus revealing weak $C(sp^3)$-H/π hydrogen bonding interaction.[19] It is important to mention that such type of interaction is also observed in solution, on account of the NOESY and ROESY NMR spectra of **2@1** in $C_2D_2Cl_4$, which reveals a clear correlation between the protons of the terminal methyl groups of the tetrasubstituted pyrene guest with the protons of the carbazolyl linker of the metallobox (see Figures S3 and S4 in Supporting Information for full details).

The solid-state structure of **2@1** reveals two possible degenerate forms on account of the tilted direction of the tetra-octynyl-pyrene relative to the metallobox. These two forms are related by a rocking motion of the trapped molecule within the metallobox suit, on account of the ^1H NMR spectrum of **2@1**, which shows one single resonance for the four lateral pyrene-CH protons of the guest (F, F′, Figure 1c), and one resonance for the pyrene-CH protons of the host (A, A′), in spite of the two sets of signals that should be expected for each group of protons for a static unsymmetrical conformation as the one displayed in the molecular structure shown in Figure 2. In order to get more information about this motion, we carried out variable temperature ^1H NMR measurements (CD_2Cl_2, 203–303 K), but the analysis of the spectra revealed that the movement is fast on the NMR timescale within all the range of temperatures used (see Figures S5–S7 in Supporting Information for details).

Considering the mechanically interlocked nature of **2@1**, it should be expected that the guest molecule is blocked

Figure 2. Two perspectives of the X-ray diffraction structure of **2@1**. Hydrogen atoms and solvent (CHCl₃) are omitted for clarity. The Figure on the bottom right shows the weak C−H/π bonding interaction between one of the hydrogen atoms of the terminal methyl group of one of the alkyl chains and one phenyl ring of the carbazolyl linker.

inside the cavity of the host, and that its release should only be possible if covalent bonds are broken. This is actually what we observed when we tried to release **2** from **2@1** by extending the heating for days, and also when we tried to encapsulate **1** into **2** by the same method (see above). These experiments suggest that the replacement of **2** by a new guest should be virtually impossible, since replacement should be accompanied by host decomposition. With this idea in mind, and considering the large association constant that we previously found for the formation of the inclusion complex coronene@**1** (4.4×10^6 M^{-1} in CD$_2$Cl$_2$),[13a] we mixed **2@1** with increasing amounts of coronene in C$_2$D$_2$Cl$_4$. Contrary to what should be expected, the monitoring of the process by ^{1}H NMR, showed that the addition of coronene to **2@1** produced the smooth replacement of **2** by coronene in the interior of the metallobox, forming coronene@**1** with the concomitant release of **2**. Interestingly, the addition of one equivalent of coronene produced equal amounts of coronene@**1** and **2@1**, thus indicating similar binding affinities for **2** and coronene with the metallobox **1** (see Figure 3). The addition of larger amounts of coronene facilitated the progressive replacement of the tetra-substituted pyrene guest **2** from the cavity of the host. For the case of the addition of five equivalents of coronene, we observed 90 % replacement of **2**, and consequently, a 9:1 molar mixture of coronene@**1** and **2@1**. Once we observed that the replacement of **2** could be achieved by adding a large polycyclic polyaromatic hydrocarbon such as coronene, we decided to study the reverse reaction, this is, the replacement of coronene in coronene@**1** by the tetrasubstituted-pyrene molecule **2**. The monitoring of this reaction by ^{1}H NMR spectroscopy showed that **2** is perfectly capable of replacing coronene from the cavity of the metallobox **1** (see Figure S11 in Supporting Information), thus in perfect fulfillment of the principle of microscopic reversibility. It needs to be mentioned, that the addition of one equivalent of **2** produced (again) equal amounts of coronene@**1** and **2@1**, therefore confirming that the guest release/uptake
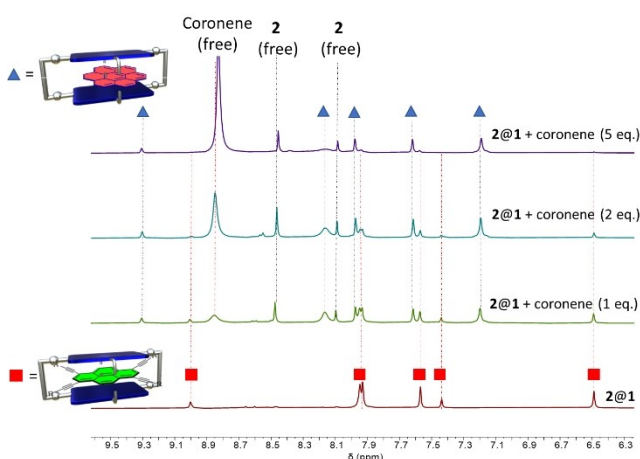
process is rapid and fully reversible (the same molar ratio is obtained for the reverse reaction), and that the equilibrium can be achieved rapidly at room temperature. Addition of increasing amounts of **2** produced the gradual replacement of coronene until complete formation of **2@1** + free coronene. This result is specially interesting because it apparently contradicts our afore mentioned observation that the pyrene guest **2** is unable to get inside the empty metallobox (Scheme 1) but, as we will explain later, the presence of coronene is crucial for facilitating the access of **2** to the cavity of **1**. In fact, this result made us consider that **2@1** should be better regarded as a pseudo-MIM (a pseudo-suitane). Once we confirmed that coronene is able to replace **2** from the cavity of **1**, we decided to study if other PAHs could also show this behaviour. We observed that mixing **2@1** with increasing amounts of perylene in C$_2$D$_2$Cl$_4$, also produced the gradual replacement of **2** from the cavity of **2@1**, although the amount of perylene needed for achieving the same degree of replacement produced by coronene was much larger (see Figure S12 in Supporting Information). For example, in this case for obtaining equal amounts of **2@1** and perylene@**2**, 10 equivalents of perylene are needed, in accordance with the smaller association constant of **1** with perylene (2.4×10^4 M^{-1} in CD$_2$Cl$_2$)[13a] compared to that with coronene.

With all these data in hand, we can draw a plausible qualitative energy profile, as the one shown in Figure 4. In the absence of coronene, the metallobox **1** does not show any ability for uptaking guest **2**. On the other hand, **2@1** does not release **2**, unless a high temperature is applied for an extended period of time, but this causes the decomposition of the metallobox. This indicates that the activation energy for the release of **1** is larger than the energy of the weakest bond that holds **2@1** together, in agreement with the mechanically interlocked nature of **2@1**. According to our previous studies on related MIMs based on (NHC)Au-(alkynyl) systems, we think that the bond that breaks first is the Au–C≡C– bond of **1**.[20] On the other hand, the metallobox **1** shows a large binding constant with coronene, and the formation of the inclusion complex coronene@**1** forms rapidly at room temperature.[13a] This indicates that coro-
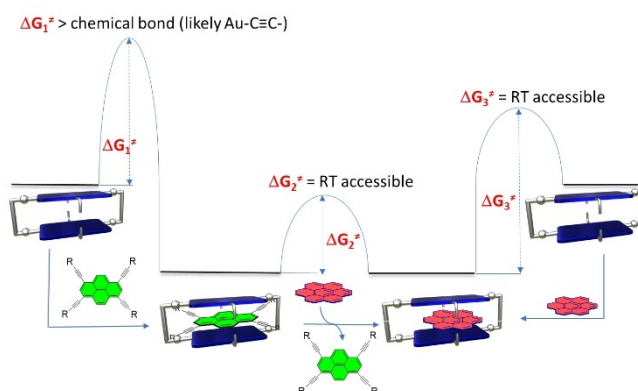

Figure 3. Selected region of the ^{1}H NMR (298 K, 500 MHz, C$_2$D$_2$Cl$_4$) spectra resulting from the mixing of **2@1** with 1, 2 and 5 equivalents of coronene (initial concentration of **2@1** = 0.5 mM).

Figure 4. Qualitative reaction profile for the process of guest release/uptake of metallobox **1** involving **2** and coronene as guests.

nene@**1** is more stable than coronene + **1**, and also that the guest uptake activation energy is accessible at room temperature. Finally, **2**@**1** and coronene@**1** can interconvert rapidly by addition of coronene to **2**@**1**, or by addition of **2** to coronene@**1**, respectively. Considering the equilibrium constant between these species, **2**@**1** and coronene@**1** must have similar ground state energies, and the rapid interconversion between them indicates a room temperature accessible activation energy.

From what is observed from this picture, we can conclude that the presence of coronene is crucial for facilitating the release/uptake process of **2**, so the next question to be solved is to know how coronene is able to release **2** from **2**@**1**. A close inspection of the molecular structure of **2**@**1** may help to unveil this question. The effective guest-accessible distance of the portal of metallobox **1** may be defined by the distance between the two hydrogens of the opposite N–H groups of the carbazolyl linkers which, after considering the van de Waals radii of the two hydrogens, measures 17.2 Å (top of Figure 5). The interlocked nature of **2**@**1** is explained because the distance between the terminal methyl groups of adjacent hexyl moieties measures 24.4 Å (after considering the van der Waals radius for each $C = 1.7$ Å), and this explains why **2** cannot pass through the portal of **1**. However, if we consider that the hexyl chains are flexible, and consider only the length of the rigid skeleton of **2**, then the guest size may go down to a minimum of 14.1 Å, measured as the distance between the two carbon atoms bound to the alkyne groups from adjacent octynyls (Figure 5).[21] This minimum guest size could be theoretically achieved if the chains of the alkyl groups folded by approaching one to each other. This leaves a range between 14.1–24.4 Å for the size of the guest, depending on whether the hexyl chains are folded and unfolded, thus the uptake/release of **2** from the metallobox **1** could, in principle, be produced for a conformation of the pyrene guest in which the alkyl chains were folded.
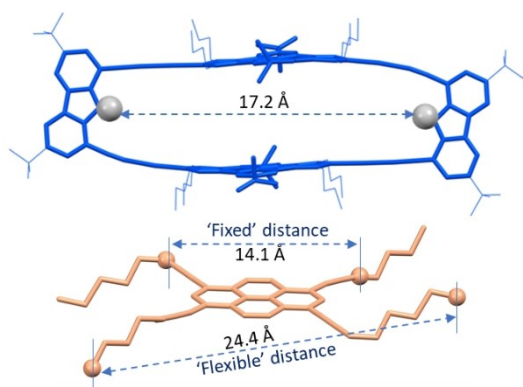

Figure 5. "Effective" host-portal and guest sizes. The effective portal size of the host is obtained by considering the distance between the two hydrogen atoms of the NH groups of the carbazolyl linkers (19.6 Å) minus the two van der Waals radii of the two hydrogen atoms (1.2 Å). The "fixed" and "flexible" distances of the guest are the measures between the two reference carbon atoms plus the two van der Waals radii of the two carbon atoms (1.7 Å).

Given that we experimentally observed that in the absence of coronene **2**@**1** cannot release **2** unless covalent bonds are broken, we must assume that, inside the metallobox, the most stable conformation of the tetra-substituted pyrene guest is the one with an open (or unfolded) conformation, i.e., the distance between the terminal carbon atoms from the neighboring alkyl chains must be larger than the guest-accessible distance of the portal of the metallobox (established as 17.2 Å, as we pointed out above). In fact, on account of NOESY and ROESY NMR experiments, we observed that, in solution, there is a direct interaction between the protons of the terminal methyl groups of the alkyl chains of the tetrasubstituted pyrene guest, and the protons of the carbazolyl linker of the metallobox, and this can only be achieved for an extended conformation of the guest when it is inside the cavity of the host. This observation also explains that the binding affinity for **2** and **1** is much larger than that reported for pyrene and **1**,[13a] since the former adds an extra estabilization provided by multiple C–H/π-interactions. With these experimental observations in hand, we thought that the explanation of the role of coronene in the unlocking of **2**@**1** should involve finding a way for which coronene facilitates the reduction of the size of **2** by folding the alkyl chains to a length that allowed it to pass through the portal of **1**.

Molecular dynamic (MD) simulations have been used extensively in the field of supramolecular chemistry, allowing to understand crucial aspects of supramolecular behaviour that cannot be approached by conventional experimental techniques. Thus, we decided to apply MD simulations with the classical MM method for exploring all possible conformational changes experienced by compound **2**, both free and inside of the metallobox. For this purpose, three different models were built: (i) free compound **2**, (ii) **2**@**1**, starting with an open (unfolded) conformer of **2** as an initial structure, and (iii) **2**@**1** starting with a closed conformer of **2** as an initial structure. In all these MD simulations, the geometry of the central region of the metallobox structure was fixed, and only the aliphatic chains attached to the flat walls consisting of aromatic rings were allowed to move. As shown in Figure 6A, results of 100 ns of MD simulations demonstrated that when acting as an isolated molecule, compound **2** is highly dynamic and the movement of its aliphatic arms is rather chaotic. The distance between the carbon atoms of the methyl groups of the reference aliphatic chains (those that determine the "Flexible distance" as shown in Figure 5) oscillates randomly and rapidly between 23–4 Å, which are the distances that can be established for the fully folded and unfolded conformers, respectively. The situation changes dramatically when the same molecule is encapsulated in **1**. In **2**@**1**, the most stable conformation, is the unfolded one, as shown in Figure 6B, with the average distance values established between two terminal carbon atoms of the aliphatic chain oscillating in a very narrow interval of around 21.4 ± 0.8 Å, and therefore well above the portal size all along the time interval. To confirm that the open conformer is the most stable one, an additional simulation was performed starting with a folded conformation of **2** (Figure 6C). For this purpose, the initial distance
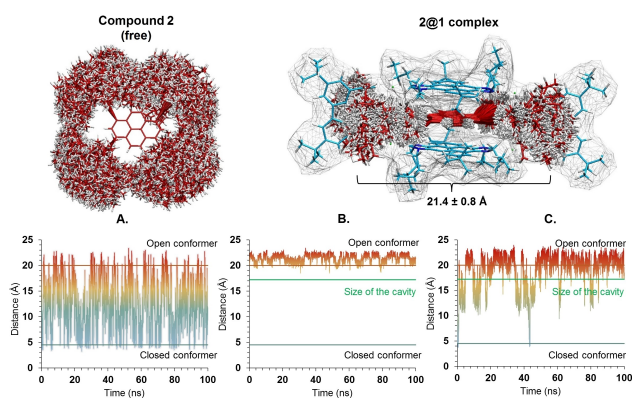
Figure 6. Conformational changes for free **2** and **2@1** represented as the evolution of the carbon-carbon distance of the terminal carbon atoms of reference aliphatic chains registered over 100 ns of the MD simulations for: A) free **2**, B) **2@1** with an open conformer of **2** as an initial structure, and (C). **2@1** with a folded conformer of **2** as an initial structure. Compound **2** is shown in red while metallobox, **1** is given in blue.

Figure 7. Evolution of carbon-carbon distance over 10 ns of the MD simulations for **2@1** without and with the presence of one (1×coronene) or two (2×coronene) coronene molecules. For clarity, compound **2**, metallobox, **1**, and coronene are shown in red, blue, and orange, respectively.

between two terminal carbons was taken to a minimum value of 4.5 Å. The results showed very fast convergence of the system to the unfolded conformation, thus supporting the higher stability of the unfolded conformation of the guest in **2@1**, as we initially hypothesized, and in agreement with our experimental observations.

As demonstrated experimentally, spontaneous release of **2** from **2@1** is only possible when coronene is added to the system. Therefore, we envisioned that the presence of coronene must somehow activate and stabilize the closed or folded conformer of **2**, which as mentioned above does not exist in the **2@1** complex. We tried to explore the possibility in which coronene interacts with long aliphatic arms of **2** and ensure the maintenance of short distances between them. First, we considered the addition of one molecule of coronene to **2@1**, and considered four possible initial orientations of coronene with respect to the aliphatic chains of the guest (see Figure S20 in Supporting Information). None of these situations yielded the closed conformation of the guest during 10 ns of explored MD simulations. However, we noticed that the molecule of coronene spontaneously trends to arrange perpendicular to the longer axle of the metallobox, establishing close contacts with two vicinal N-butyl chains of the N-heterocyclic carbenes, with one of the hydrogen atoms of coronene oriented towards the hydrogen of the N–H group of one of the carbazolyl linkers (Figure S20.IV). This renders a half-closed conformation of the guest, with an average C–C distance of terminal carbons oscillating in a narrow interval of 14.2 ± 1.0 Å, as shown in Figure 7. In principle, this distance is already sufficiently small to allow compound **2** to pass the narrow gate formed by the two hydrogen atoms of the NH groups of the carbazolyl linkers of the host. We think that this orientation of the molecule of coronene is favored by multiple C–H/π interactions between the C–H bonds of the *n*-But groups of the metallobox and the polyconjugated surface of the molecule of coronene. This specific coronene
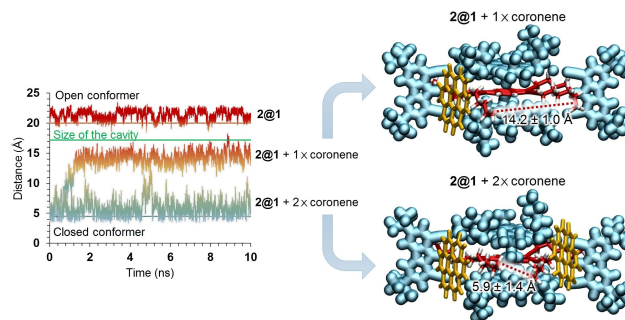
orientation towards compound **2@1** inspired an alternative possibility in which not one but two coronene molecules of coronene are involved in interactions with the aliphatic chains of compound **2**. This new scenario resulted in a stable conformer with an average C–C distance of the terminal methyl groups oscillating in an interval of 5.9 ± 1.4 Å (See Figure 7), therefore suggesting that the presence of two coronene molecules significantly increases the possibility of releasing 2 from **2@1**.

We wanted to see if we could give further experimental support to these computational studies. The key point is to find if, in solution, there is any kind of interaction between a molecule of free coronene and the hydrogen atoms of the N–H group of the carbazolyl linkers. For this purpose, we performed NOESY and ROESY NMR experiments for mixtures of **2@1** and coronene in CD_2Cl_2 (Figures S13 and S14). These experiments revealed two important facts: *i)* there is a clear correlation between the resonances due to the protons of free coronene and the signals due to the NH proton of the carbazolyl linker of the metalobox, and *ii)* the correlation between the protons of the terminal methyl groups of the tetrasubstituted pyrene and the resonances due to the carbazolyl linger are no longer observed. These observations give clear support to the computational calculations, as they srtongly suggest that free coronene interacts directly with the NH proton of the carbazolyl linker, and that the conformation of the tetrasubstituted pyrene is no longer extended (unfolded) when coronene is present in the solution.

Conclusion

In summary, we described a mechanically interlocked molecule (MIM) comprising a tetragold metallobox and a tetraoctynyl-pyrene guest that can be regarded as a metallosuit[4]ane. The mechanically interlocked nature of **2@1** is confirmed mainly by two facts: i) guest **2** cannot be released from **2@1** unless covalent bonds are broken, and ii) mixing **2** and **1** does not allow the formation of **2@1**, even

when high temperatures and very long reaction times are used.

The fact that the addition of coronene allows the smooth release of **2** from **2@1** seems contradictory with the fact that **2@1** is a mechanically interlocked molecule, and therefore, it may be more appropriate to consider this suitane-like species as an extreme case of a kinetically stable entity or, as we state in the title of this study, a (pseudo)-MIM (a pseudo-suitane). Our studies suggest that the cooperative action of two molecules of coronene facilitates the formation of a narrow corridor which is fixed to the metallobox in a manner that the flexible arms of the guest are compressed, so that they can adopt a folded conformation whose size is able to pass smoothly through the portal of the host. This means that coronene can be regarded as a *shoehorn*, in the sense that it is able to help the guest to slide in and out the metallobox. We think that this type of hetero-guest assisted MIM unlocking, or more graphically expressed as "*shoe-horning*" effect, has never been described before, and this makes us foresee that this effect may have important implications in future supramolecular chemistry studies.

Conflict of Interest

The authors declare no conflict of interest.

Data Availability Statement

The data that support the findings of this study are available in the Supporting Information of this article.

[1] a) F. Liu, H. Wang, K. N. Houk, *Curr. Org. Chem.* **2013**, *17*, 1470–1480; b) S. Rieth, K. Hermann, B. Y. Wang, J. D. Badjic, *Chem. Soc. Rev.* **2011**, *40*, 1609–1622.

[2] K. N. Houk, K. Nakamura, C. M. Sheu, A. E. Keating, *Science* **1996**, *273*, 627–629.

[3] Y. S. Byun, O. Vadhat, M. T. Blanda, C. B. Knobler, D. J. Cram, *J. Chem. Soc. Chem. Commun.* **1995**, 1825–1827.

[4] K. Hermann, Y. Ruan, A. M. Hardin, C. M. Hadad, J. D. Badjic, *Chem. Soc. Rev.* **2015**, *44*, 500–514.

[5] J. B. Bruns, J. F. Stoddart, *The Nature of the Mechanical Bond: From Molecules to Machines*, Wiley, Hoboken, **2016**.

[6] a) S. A. Nepogodiev, J. F. Stoddart, *Chem. Rev.* **1998**, *98*, 1959–1976; b) J. P. Sauvage, *Acc. Chem. Res.* **1998**, *31*, 611–619; c) M. Fujita, *Acc. Chem. Res.* **1999**, *32*, 53–61; d) N. H. Evans, P. D. Beer, *Chem. Soc. Rev.* **2014**, *43*, 4658–4683; e) G. Gil-Ramírez, D. A. Leigh, A. J. Stephens, *Angew. Chem. Int. Ed.* **2015**, *54*, 6110–6150; *Angew. Chem.* **2015**, *127*, 6208–6249; f) S. Mena-Hernando, E. M. Perez, *Chem. Soc. Rev.* **2019**, *48*, 5016–5032; g) J. D. Crowley, S. M. Goldup, A. L. Lee, D. A. Leigh, R. T. McBurney, *Chem. Soc. Rev.* **2009**, *38*, 1530–1541; h) W. L. Shan, Y. J. Lin, F. E. Hahn, G. X. Jin, *Angew. Chem. Int. Ed.* **2019**, *58*, 5882–5886; *Angew. Chem.* **2019**, *131*, 5941–5946.

[7] a) G. Wenz, B. H. Han, A. Muller, *Chem. Rev.* **2006**, *106*, 782–817; b) B. Taghavi Shahraki, S. Maghsoudi, Y. Fatahi, N. Rabiee, S. Bahadorikhalili, R. Dinarvand, M. Bagherzadeh, F. Verpoort, *Coord. Chem. Rev.* **2020**, *423*, 213484; c) A. Martinez-Cuezva, F. Morales, G. R. Marley, A. Lopez-Lopez, J. Carlos Martinez-Costa, D. Bautista, M. Alajarin, J. Berna, *Eur. J. Org. Chem.* **2019**, 3480–3488.

[8] a) Z. Ashbridge, S. D. P. Fielden, D. A. Leigh, L. Pirvu, F. Schaufelberger, L. Zhang, *Chem. Soc. Rev.* **2022**, *51*, 7779–7809; b) S. L. Huang, T. S. A. Hor, G. X. Jin, *Coord. Chem. Rev.* **2017**, *333*, 1–26; c) W. X. Gao, H. J. Feng, B. B. Guo, Y. Lu, G. X. Jin, *Chem. Rev.* **2020**, *120*, 6288–6325.

[9] a) D. A. Leigh, J. K. Y. Wong, F. Dehez, F. Zerbetto, *Nature* **2003**, *424*, 174–179; b) J. M. Abendroth, O. S. Bushuyev, P. S. Weiss, C. J. Barrett, *ACS Nano* **2015**, *9*, 7746–7768; c) J. P. Sauvage, *Angew. Chem. Int. Ed.* **2017**, *56*, 11080–11093; *Angew. Chem.* **2017**, *129*, 11228–11242; d) D. Sluysmans, J. F. Stoddart, *Trends Chem.* **2019**, *1*, 185–197; e) Q. H. Guo, Y. Y. Qiu, X. Y. Kuang, J. Q. Liang, Y. N. Feng, L. Zhang, Y. Jiao, D. K. Shen, R. D. Astumian, J. F. Stoddart, *J. Am. Chem. Soc.* **2020**, *142*, 14443–14449; f) J. F. Stoddart, *Angew. Chem. Int. Ed.* **2017**, *56*, 11094–11125; *Angew. Chem.* **2017**, *129*, 11244–11277.

[10] a) L. van Dijk, M. J. Tilby, R. Szpera, O. A. Smith, H. A. P. Bunce, S. P. Fletcher, *Nat. Chem. Rev.* **2018**, *2*; b) R. W. Heard, J. M. Suarez, S. M. Goldup, *Nat. Chem. Rev.* **2022**, *6*, 182–196.

[11] a) M. J. Chmielewski, J. J. Davis, P. D. Beer, *Org. Biomol. Chem.* **2009**, *7*, 415–424; b) M. J. Langton, P. D. Beer, *Acc. Chem. Res.* **2014**, *47*, 1935–1949.

[12] a) K. K. Cotí, M. E. Belowich, M. Liong, M. W. Ambrogio, Y. A. Lau, H. A. Khatib, J. I. Zink, N. M. Khashab, J. F. Stoddart, *Nanoscale* **2009**, *1*, 16–39; b) Z. Luo, X. W. Ding, Y. Hu, S. J. Wu, Y. Xiang, Y. F. Zeng, B. L. Zhang, H. Yan, H. C. Zhang, L. L. Zhu, J. J. Liu, J. H. Li, K. Y. Cai, Y. L. Zhao, *ACS Nano* **2013**, *7*, 10271–10284; c) J. Riebe, J. Niemeyer, *Eur. J. Org. Chem.* **2021**, 5106–5116.

[13] a) S. Ibáñez, E. Peris, *Angew. Chem. Int. Ed.* **2020**, *59*, 6860–6865; *Angew. Chem.* **2020**, *132*, 6927–6932; b) S. Ibáñez, D. G. Gusev, E. Peris, *Organometallics* **2020**, *39*, 4078–4084.

[14] a) Z. J. Zhang, M. J. Zaworotko, *Chem. Soc. Rev.* **2014**, *43*, 5444–5455; b) J. E. Beves, B. A. Blight, C. J. Campbell, D. A. Leigh, R. T. McBurney, *Angew. Chem. Int. Ed.* **2011**, *50*, 9260–9327; *Angew. Chem.* **2011**, *123*, 9428–9499; c) T. J. Hubin, D. H. Busch, *Coord. Chem. Rev.* **2000**, *200*, 5–52; d) R. Hoss, F. Vogtle, *Angew. Chem. Int. Ed. Engl.* **1994**, *33*, 375–384; *Angew. Chem.* **1994**, *106*, 389–398; e) S. Anderson, H. L. Anderson, J. K. M. Sanders, *Acc. Chem. Res.* **1993**, *26*, 469–475; f) M. Denis, S. M. Goldup, *Nat. Chem. Rev.* **2017**, *1*, 0061.

[15] a) A. R. Williams, B. H. Northrop, T. Chang, J. F. Stoddart, A. J. P. White, D. J. Williams, *Angew. Chem. Int. Ed.* **2006**, *45*, 6665–6669; *Angew. Chem.* **2006**, *118*, 6817–6821; b) X.-Y. Chen, D. Shen, K. Cai, Y. Jiao, H. Wu, B. Song, L. Zhang, Y.

Angew. Chem. **2023**, *135*, e202301914 (7 of 8)

© 2023 The Authors. Angewandte Chemie published by Wiley-VCH GmbH

Tan, Y. Wang, Y. Feng, C. L. Stern, J. F. Stoddart, *J. Am. Chem. Soc.* **2020**, *142*, 20152–20160.

[16] D. Nuevo, M. Poyatos, E. Peris, *Organometallics* **2018**, *37*, 3407–3411.

[17] a) A. J. Stasyuk, O. A. Stasyuk, M. Sola, A. A. Voityuk, *J. Mater. Chem. C* **2021**, *9*, 9436–9445; b) Y. Wu, Q. H. Guo, Y. Y. Qiu, J. A. Weber, R. M. Young, L. Bancroft, Y. Jiao, H. L. Chen, B. Song, W. Q. Liu, Y. N. Feng, X. G. Zhao, X. S. Li, L. Zhang, X. Y. Chen, H. Li, M. R. Wasielewski, J. F. Stoddart, *Proc. Natl. Acad. Sci. USA* **2022**, *119*; c) H. Y. Xu, M. D. Lin, J. Yuan, B. Y. Zhou, Y. X. Mu, Y. P. Huo, K. L. Zhu, *Chem. Commun.* **2021**, *57*, 3239–3242; d) K. L. Zhu, G. Baggi, V. N. Vukotic, S. J. Loeb, *Chem. Sci.* **2017**, *8*, 3898–3904; e) A. Pun, D. A. Hanifi, G. Kiel, E. O'Brien, Y. Liu, *Angew. Chem. Int. Ed.* **2012**, *51*, 13119–13122; *Angew. Chem.* **2012**, *124*, 13296–13299; f) T. Chang, A. M. Heiss, S. J. Cantrill, M. C. T. Fyfe, A. R. Pease, S. J. Rowan, J. F. Stoddart, D. J. Williams, *Org. Lett.* **2000**, *2*, 2943–2946; g) W. Q. Liu, C. L. Stern, J. F. Stoddart, *J. Am. Chem. Soc.* **2020**, *142*, 10273–10278.

[18] Deposition Number 2193393 contains the supplementary crystallographic data for this paper. These data are provided free of charge by the joint Cambridge Crystallographic Data Centre and Fachinformationszentrum Karlsruhe Access Structures service.

[19] a) M. Nishio, *CrystEngComm* **2004**, *6*, 130–158; b) M. Nishio, Y. Umezawa, K. Honda, S. Tsuboyama, H. Suezawa, *CrystEngComm* **2009**, *11*, 1757–1788; c) M. Nishio, *Phys. Chem. Chem. Phys.* **2011**, *13*, 13873–13900.

[20] S. Ibáñez, C. Vicent, E. Peris, *Angew. Chem. Int. Ed.* **2022**, *61*, e202112513; *Angew. Chem.* **2022**, *134*, e202112513.

[21] It is also important to point out that this minimum distance of 14.1 Å can even be smaller if we also considered the small deviations of the C(ar)-C(ar)-C(alkyne) angle from the ideal 120°, and the small deviations of the alkyne substituent from linearity.